A new framework for modelling the dynamics and the breakage of capsules, vesicles and cells in fluid flow

Alexiadis, Alessio

DOI:
10.1016/j.piutam.2015.03.010

Document Version
Publisher's PDF, also known as Version of record

Citation for published version (Harvard):
Alexiadis, A 2015, 'A new framework for modelling the dynamics and the breakage of capsules, vesicles and cells in fluid flow', *IUTAM Procedia*, vol. 16, pp. 80-88. https://doi.org/10.1016/j.piutam.2015.03.010

Available online at www.sciencedirect.com

ScienceDirect

Procedia IUTAM 16 (2015) 80 – 88

Procedia IUTAM

www.elsevier.com/locate/procedia

IUTAM Symposium on Dynamics of Capsules, Vesicles and Cells in Flow

A new framework for modelling the dynamics and the breakage of capsules, vesicles and cells in fluid flow

Alessio Alexiadis[a]*

[a]*School of Chemical Engineering, University of Birmingham, B15 2TT United Kingdom*

Abstract

This paper proposes a model based on the combination of smoothed particle hydrodynamics (SPH) and coarse-grained molecular dynamics (CGMD) for the simulation of flexible particles, such as capsules, vesicles or cells, under various flow conditions. The model can deal with both breakable and unbreakable particles. Validation against data available in the literature is included, and results concerning shear and Poiseuille flow in the presence of obstacles or sharp objects are discussed.

Peer-review under the responsibility of the organizing committee of DYNACAPS 2014 (Dynamics of Capsules, Vesicles and Cells in Flow).

Keywords: Smoothed particle hydrodynamics; Coarse-grained molecular dynamics; Flexible cells; Breakable cells, Solid-liquid interaction

1. Introduction

There are many established numerical techniques, such as Computational Fluid Dynamics (CFD), Lattice-Boltzmann (LB) or Boundary Integral Methods (BIM), that are used for simulating solid-liquid flows when the dispersed phase is constituted of flexible and deformable particles, but none of these methods, by themselves, can handle breakable particles. This limitation is particular relevant in certain industrial processes, where encapsulated soft particles (e.g. cells, vesicles and capsules) are disrupted by induced flows; examples can be found in high pressure homogenization [1], flow induced cell disruption [2] or high-shear mechanical methods [3].

In order to overcome these shortcomings, a new, hybrid, approach, based on the combination of smoothed particle hydrodynamics (SPH) and coarse-grained molecular dynamics (CGMD), is proposed here. Hybrid models combining together SPH and MD have been proposed in the past [4], but with a completely different philosophy and aim. Previous studies have focused on simulations, where a macroscopic SPH-region interacts with a separate

* Corresponding author. Tel.: +44 (0) 121 414 5305.
E-mail address: a.alexiadis@bham.ac.uk

Peer-review under the responsibility of the organizing committee of DYNACAPS 2014 (Dynamics of Capsules, Vesicles and Cells in Flow).
doi:10.1016/j.piutam.2015.03.010

microscopic MD-region. Here, we are not focusing on the actual molecular structure of the flow, but rather on a coarse-grained ball-and-spring representation of elastic solids, which coexists in the same domain with a SPH representation of the fluid. More details concerning the differences between the hybrid approach used in this paper and previous SPH-MD hybrids can be found in [5], while specific discussion of available computational methods for flows containing cells, capsules and vesicles can be found in [6–9].

This paper is organized as follows: initially a brief overview of SPH and CGMD is given and the interaction between the fluid (SPH) and the flexible boundaries (CGMD) is explained. Subsequently, the effect of various flow conditions and external geometries on the vesicles dynamics is discussed. Finally, validation with experimental and numerical data available in the literature is presented.

2. SPH fundamentals

This section gives a brief introduction of SPH for fluids, more information can be found in [4]. The SPH equations of motion are obtained by the discrete approximations of the Navier-Stokes equation at a set of points, which can be thought of as particles characterized by their own mass, velocity, pressure and density. The fundamental idea behind this discrete approximation lies in the mathematical identity

$$f(\mathbf{r}) = \iiint f(\mathbf{r}')\delta(\mathbf{r}-\mathbf{r}')\mathbf{dr}', \tag{1}$$

where $f(\mathbf{r})$ is a generic function defined over the volume V, the vector $\mathbf{r}$ is a three-dimensional point in V and $\delta(\mathbf{r})$ is the three-dimensional delta function. In the SPH formalism, the delta function is approximated by a function W called the smoothing kernel with a characteristic width h (smoothing length) such that

$$\lim_{h\to 0} W(\mathbf{r}, h) = \delta(\mathbf{r}). \tag{2}$$

This brings the approximation

$$f(\mathbf{r}) \approx \iiint f(\mathbf{r}')W(\mathbf{r}-\mathbf{r}', h)\mathbf{dr}', \tag{3}$$

which can be discretised over a series of particles of mass $m = \rho(\mathbf{r})\mathbf{dr}$ obtaining

$$f(\mathbf{r}) \approx \sum_i \frac{m_i}{\rho_i} f(\mathbf{r}_i)W(\mathbf{r}-\mathbf{r}_i, h), \tag{4}$$

where $f(\mathbf{r_i})$, m_i and ρ_i are the mass and density of the i^{th} particle, and i ranges over all particles within the smoothing kernel. Equation (4) represents the discrete approximation of a generic continuous field and can be used to approximate the Navier-Stokes equation

$$\frac{d\mathbf{v}_i}{dt} = \sum_j m_j \left(\frac{P_i}{\rho_i^2} + \frac{P_j}{\rho_j^2} + \Pi_{i,j}\right)\nabla_j W_{i,j} + \mathbf{f}_i, \tag{5}$$

where v_i is the velocity of particle i, $W_{i,j}$ means $W(\mathbf{r_j}\text{-}\mathbf{r_i}, h)$, ∇_j denotes the gradient of the kernel with respect of the coordinate r_j, P is the pressure, $\mathbf{f}_i$ a volumetric body force, and $\Pi_{i,j}$ introduces the viscous forces. Various expressions for the tensor $\Pi_{i,j}$ are available in the literature. Here we use the Morris' formulation for low Reynolds numbers [10]. At each time step, (5) is used to update the velocities of the fluid particle, while their density can be calculated either by (3), considering ρ as a normal scalar field, or, as done in this work, by means of the discrete approximation of the continuity equation

$$\frac{d\rho_i}{dt} = \sum_j m_j \mathbf{v}_{i,j}\nabla_j W_{i,j}, \tag{6}$$

where $\mathbf{v}_{i,j}=\mathbf{v}_i-\mathbf{v}_j$.
The equation of motion of the SPH particles follows from (5):

$$m_i \frac{d^2\mathbf{r}_i}{dt^2} = \sum_j m_i m_j \left(\frac{P_i}{\rho_i^2} + \frac{P_j}{\rho_j^2} + \Pi_{i,j}\right) \nabla_j W_{i,j} + \mathbf{f}_i. \quad (7)$$

In its original version, the SPH method was derived for compressible flows. Incompressible, and computationally more expensive, versions have been subsequently proposed, but in many practical cases, the "weakly-compressible approximation" is acceptable. Density variations, in fact, can be estimated as

$$\frac{\delta\rho}{\rho} = \frac{VL}{\tau c^2}, \quad (8)$$

where L is the characteristic length scale of the flow, τ the characteristic time scale, V the velocity and c the speed of sound in the medium. This means that for problems at low Mach number, the weakly-compressible approach brings only small density variations and can be safely used. The weakly-compressibility requires an equation of state. In this paper, we use Tait's equation of state, which has been specifically devised to model water

$$P(\rho) = \frac{c_0\rho_0}{7}\left[\left(\frac{\rho}{\rho_0}\right)^7 - 1\right], \quad (9)$$

where c_0 and ρ_0 are, respectively the sound speed and density at zero applied stress.

3. Coarse-Grained Molecular Dynamics

Molecular dynamics is a form of investigation where the motion and the interaction of a certain number of computational atoms or molecules are studied. In classical MD simulations atoms move according to the Newtonian equations of motion

$$m_i \frac{d^2\mathbf{r}_i}{dt^2} = -\frac{\partial}{\partial\mathbf{r}} U_{tot}(\mathbf{r}_1, \mathbf{r}_2, \ldots \mathbf{r}_N), \quad (10)$$

where U_{tot} is the total interatomic potential, which can be divided into two main parts: non bonded and intramolecular. Non bonded forces are usually represented by the so-called Lennard-Jones potential, while the intramolecular forces are often divided in subgroups

$$U_{intramolecular} = U_{bond} + U_{angle} + U_{dihedral}. \quad (11)$$

Each of these potentials can have different forms. In this study, we only consider harmonic potentials:

$$U_{bond} = k_b(r - r_0)^2, \quad (12)$$

where k_b a Hookean coefficient and r_0 an equilibrium distance,

$$U_{angle} = k_a(\theta - \theta_0)^2, \quad (13)$$

where k_a is an angular Hookean coefficient and θ_0 an equilibrium angle,

$$U_{dihedral} = k_d(\phi - \phi_0)^2, \quad (14)$$

where k_d is a torsional Hookean coefficient and ϕ_0 an equilibrium dihedral angle (discussed below).
Equations (12─14) are the basis for the ball-and-stick representation of molecules that can be coarse-grained to model macroscopic solids (see Figure 1).

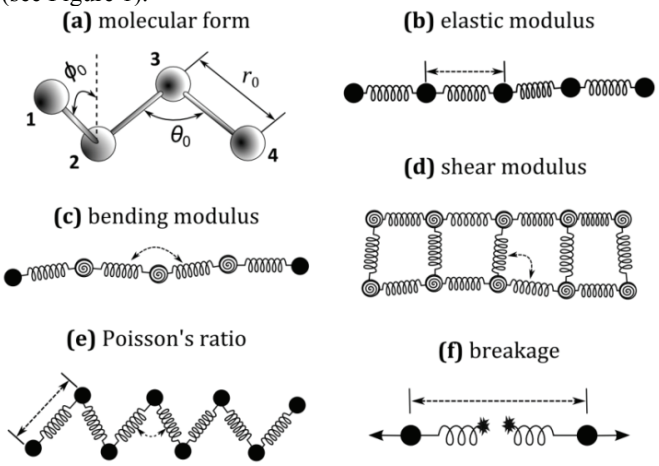

Figure 1. The molecular dynamics approach is coarse-grained to model macroscopic solids.

Figure 1a illustrates the molecular foundation of (12─14). Atoms belonging to a certain molecule are bonded together by means of forces, which tend to maintain two atoms at a certain specific distance r_0 in (12), three atoms at a certain specific angle θ_0 in (13) and four atoms at a certain specific dihedral angle ϕ_0 in (14). The dihedral, or torsional, angle is the angle between the two planes generated by atoms 1-2-3 and atoms 2-3-4 in Figure 1a.

This approach can be coarse-grained and employed to model macroscopic phenomena such as stretching and bending of cellular membranes under the effect of external forces. The elastic modulus (Figure 1b) is connected to (12) by considering coarse-grained portions (pseudo-particles) of the solid instead of atoms. The bending modulus can be achieved by considering (13) acting on a sort of 'hinge' as illustrated in Figure 1c. In order to simulate the effect of shear, the membrane can be coarse-grained with more than one layer of particles and (13) applied to the internal angles as indicated in Figure 1d. A similar approach can be employed for the Poisson's Ratio. This time, however, the two layers of particles should be arranged with a different disposition like the one shown in Figure 1e. Breakage can also be included by assuming that, if the distance between two particles exceeds a certain maximum value r_{max}, the bond is broken and the two particles separated. Finally, torsion can be modelled by considering a coarse-grained dihedral potential (14) on the particles forming the membrane.

Figure 1 illustrates the strategies that can be used to simulate various macroscopic solids with coarse-grained molecular potentials. These strategies, moreover, can be combined together in order to reflect the whole array of phenomena indicated in Figure 1. We can use, for instance, (12) for simulate the membrane elastic modulus and two sets of angular potentials (13), one for modelling the bending modulus (Figure 1c) and another for the shear modulus (Figure 1d). It is also important to highlight the fact that the harmonic potentials used in (12─14) are only one of all the possible ways of representing the forces between particles. In this article harmonic/hookean forces are considered for their simplicity, but more complicated potentials such as FENE, Morse or quartic can be easily introduced in the model.

4. Coupling between SPH and CGMD

The interaction between the solid (CGMD particles) and the liquid (SPH particles) is defined by boundary conditions, which relate the behaviour of two adjacent materials at the common interface. There are three main types of phenomena that must be taken into consideration in designing these boundary conditions [11]: no-penetration, no-

slip and continuity of stresses. In continuum mechanics, these conditions are often represented as

$$\left(\frac{\partial}{\partial t}\mathbf{u} - \mathbf{v}\right) \cdot \mathbf{n} = 0 \text{ (no} - \text{penetration)}, \tag{15}$$

$$\left(\frac{\partial}{\partial t}\mathbf{u} - \mathbf{v}\right) \times \mathbf{n} = 0 \text{ (no} - \text{slip)} \tag{16}$$

and

$$\sigma_s \mathbf{n} = \sigma_f(-\mathbf{n}) \text{(continuity of stresses)} \tag{17}$$

where **n** is the normal to the boundary, **u** the displacement of the solid, **v** the velocity of the liquid, σ_s the stresses in the solid and σ_f in the fluid.

In the particle framework, the no-penetration conditions is often implemented by means of an additional central force with a Lennard-Jones form

$$f(r) = K\left[\left(\frac{r^*}{r}\right)^{p_1} - \left(\frac{r^*}{r}\right)^{p_2}\right]\frac{\mathbf{r}}{r^2}, \tag{18}$$

where r^* represents the repulsive radius of the particle, and p_1 and p_2 are usually set to 4 and 2, although also the original 12-6 Lennard-Jones values are sometimes used. The constant K has the units of V^2 and is often chosen on the basis of a characteristic velocity of the flow. The no-slip condition models the friction between the solid and the fluid. In finite-element numerical methods it is often enforced by imposing that the two materials have the same velocity at the interface. In our SPH-CGMD framework, a similar strategy can be achieved by superimposing a fluid ghost particle above the solid particles at the interface. The advantage of using a particle-particle representation is that, once both the no-penetration and no-slip boundary condition are enforced, the continuity of stress is automatically satisfied by the equation of motion (5).

5. Results

Here, results concerning the deformation and breakage of capsules under various flow conditions are shown. The effect of both shear- and gravity-driven flow is considered together with the interaction of the particles with obstacles or sharp objects that may pierce their protective membrane. The particles are designed as 'pouches' with a liquid content. The external membrane represents the solid phase, where the CGMD framework is used, while both the internal and external liquids are represented by SPH particles. For simplicity, in these simulations, it is assumed that the density of the membrane of both liquids (inside and outside cell's membrane) is the same. The domain is a 2D rectangular channel with length $L = 4 \cdot 10^{-4}$ m and thickness $D = 10^{-4}$ m (Figure 2).

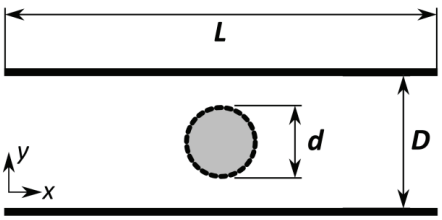

Figure 2. The computational domain with a flexible vesicle (initially circular) in the centre.

The liquid is divided in 2048 fluid particles (61 inside the membrane) with a mass $m = 2.5 \cdot 10^{-8}$ kg initially located at a distance $\Delta L = 5 \cdot 10^{-6}$ m. The membrane is discretized with 48 particles. The density of the liquid is $\rho = 1000$ kg m-

^{3}, the viscosity $\mu = 0.1$ kg m^{-1} s^{-1}, the smoothing length $h = 1.18 \cdot 10^{-5}$ m, $r_0 = 3.3 \cdot 10^{-6}$ m , $k_b = 10$ J m^{-2}; $\theta_0 = 172.5$ rad, $k_a = 10^{-18}$ J, only one layer of particles is used to model the membrane and no dihedral potential is considered (the effect of Poisson's ratio, shear and torsional modulus is therefore neglected); the L-J parameters used for the solid-liquid interaction (eq. 18) are $\sigma = \Delta L$ and $K = 10^{-12}$ J, when breakage of the membrane is considered, this occurs when the distance between two solid particles exceeds r_0 by 10%. Here, these values were chosen without a specific application in mind. In general, they should be derived by experimental data or other available information on the cells. Boundary conditions in the x direction are periodic. This means that when a particle exits the channel from one end, it re-enters from the opposite end. The first case examined (Figure 3) is shear flow. A flexible particle is placed in a 2D channel, whose upper wall is put in motion with a velocity $v_w = 2 \cdot 10^{-3}$ m s^{-1}. The lower wall is not moving and the velocity difference between the two walls creates a velocity gradient. The soft particle is subjected to a strong shear flow, which initially deforms its shape. After 0.1s, no further evolution of the shape was observed. The particle, however, rotates clockwise, which is consistent with the presence of a velocity gradient. In Figure 4, the same simulation is repeated for a breakable particle. As already mentioned, if the elongation of the spring between two of the pseudo-particles forming the capsule membrane exceeds 10% of r_0, the bond breaks and the content of the capsule is released in the liquid. Rupture of the membrane is observed at around $t = 0.1$s in our simulations. Qualitatively, this case is typical of applications such as airlift bioreactors or flow-induced cells disruption where flow circulation generates shear stresses that can lead to cells breakage.

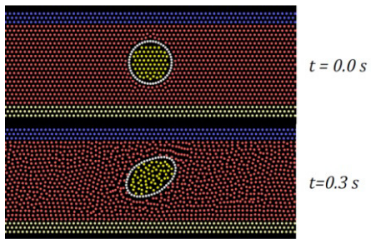

Figure 3. Flexible particle in shear flow.

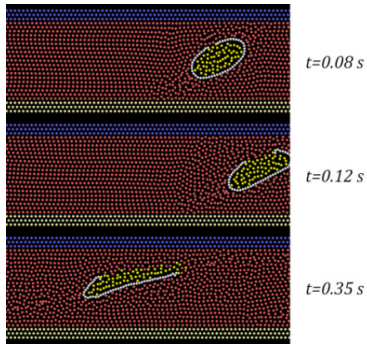

Figure 4. Breakable particle in shear flow.

Another situation examined involves gravity-driven flow with an obstacle. In this case, the flow is driven by a volumetric, gravity-like force in the x direction $g = 1$ m s^{-2} and both walls are stationary. Towards the end of the channel, the lumen is reduced to 40 mm by the presence of an obstacle. Two simulations are carried out: one with an unbreakable particle (Figure 5) and the other with a breakable particle (Figure 6). An unbreakable particle squeezes in the space between the wall and the obstacle. The main mechanical stresses on the external membrane of the particle come from the interaction with both the upper wall and the obstacle. This, in the case of a breakable particle, creates two breaking points in the membrane structure.

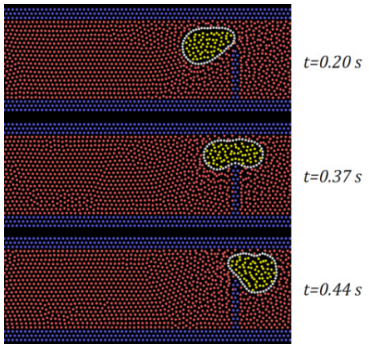

Figure 5. Flexible particle with obstacle.

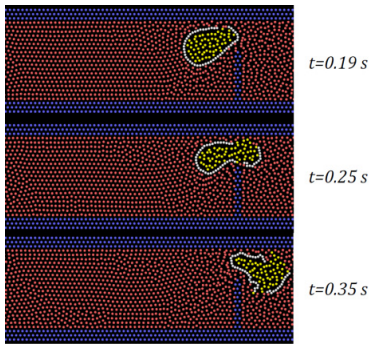

Figure 6. Breakable particle with obstacle.

In Figure 7 the collision with a sharp object is taken into consideration. In this simulation, the flow is gravity-driven as in the previous case, but a sharp object is added at the end of the channel. In this case, only breakable particles are considered. The flow pushes the particle towards the sharp object. Initially, the particle deforms, but above a certain pressure the sharp object pierces the external membrane and the internal liquid is released into the main flow. The last section of Figure 7 (t = 1s) shows some yellow particles, coming from the interior of the capsule, on the left of the channel. This is simply due to the periodic boundary conditions in the x direction. In practical applications, this case can be used for the simulation of processes where the cell walls are cut by an external sharp object.

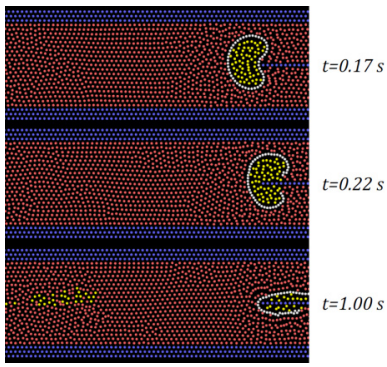

Figure 7. Breakable particle with sharp object.

6. Qualitative validation

So far the model has been used to simulate extreme conditions characterized by unconventional geometries and membrane rupture. This has been done on purpose in order to highlight its main advantages and, in particular, the fact that breakage can be easily simulated with our hybrid method.

In this section, however, we compare the shape of flexible vesicles in Poiseuille flow obtained with our method and results, both numerical and experimental, available in the literature [12─15]. These examples have been included to demonstrate the consistency of our methodology with available literature results, but extensive validation involving the full shape-diagram of vesicles in Poiseuille (or other) flow is beyond the scope of the present study.
Generally, results are classified according to specific dimensionless groups such as the Capillary Number, which in our framework can be defined as

$$Ca = \frac{\mu V_{//}^2}{k_a}, \tag{19}$$

the Confinement Number

$$R = \frac{d}{D}, \tag{20}$$

and the Reduced Volume Number

$$v = \frac{3\mathcal{V}}{4\pi\left(\frac{\mathcal{S}}{4\pi}\right)^{3/2}}, \tag{21}$$

where $\mathcal{V}$ is the vesicle volume and $\mathcal{S}$ the membrane area. Numerical methods traditionally used in fluid/cell simulations (e.g. boundary integral method) require a constant cell's volume and surface area. Cell deformability, therefore, is linked to the initial (and constant) deflation indicated by the reduced volume (see [12]). This device, however, is not necessary with the method proposed here. Deformability, in fact, is directly related to the elasticity of the membrane expressed by the Hooke constant k_b. Instead of the reduced volume, therefore, a more indicative dimensionless number for our case would be the Cauchy Number

$$C = \frac{\rho V^2 r_0}{n k_b}. \tag{22}$$

The term n (number of particles used to simulate the membrane) is necessary in eq. 22 to account for the overall elastic resistance of the membrane (otherwise C would depend on the discretization adopted).

Two simulations are carried out at conditions similar, but not identical to Section 5. In order to provide more details on the resulting particle's shape, in fact, a double number of particles, which basically means a double overall resolution, has been used in these simulations. The membrane is now discretized with 98 particles and θ_0 = 176.33. The particle was assumed unbreakable and the channel thickness reduced to 70 μm. The first simulation was run with $k_a = 2{\cdot}10^{-12}$ J and k_b = 10 J m^{-2}, the second with $k_a = 2{\cdot}10^{-14}$ J and k_b = 0.1 J m^{-2}. Except for these differences, the simulations in Figure 8 were run at the same conditions indicated in Section 5.

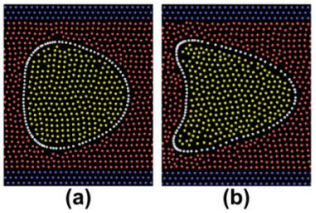

Figure 8. Bullet and parachute shapes.

The results illustrated in Figure 8 are for R =0.7 and, respectively, Ca = 0.001 and $C = 2.5{\cdot}10^{-15}$ (Figure 8a), and Ca = 0.1 and $C = 2.5{\cdot}10^{-13}$ (Figure 8b). The outcome of the simulations can be compared with both experimental and numerical results available elsewhere [8-11]. The model correctly predicts the formation of the so-called 'bullet' and 'parachute' shapes and results are consistent with those reported in the literature. The comparison is here limited to two specific cases; a more systematic validation can be achieved by considering a larger range of flow conditions. The main goal of this paper, however, is to highlight the potential of the method especially when breakage is involved.

7. Conclusions

This article introduces a new SPH-CGMD hybrid framework for the simulation of elastic, deformable and breakable

vesicles, cells, and capsules under various flow conditions. This approach shows a clear advantage over other techniques in the case of flows containing breakable particles. The main goal of this paper is to offer an initial demonstration of the method and show its potential. In the future, the model can be improved in various directions. It would be very interesting, for instance, to include merging of surfactants' vesicles.

It is also important to highlight that, despite the fact that this technique is based on a hybrid framework, both SPH and CGMD have a common discrete nature, which allows a very efficient numerical coupling. Moreover, the supporting theory it not overly complicated and any researcher with a working knowledge of either MD or SPH will soon feel comfortable working with it.

References

1. Spiden EM, Yap BHJ, Hill DRA, Kentish SE, Scales PJ, Martin GJO. Quantitative evaluation of the ease of rupture of industrially promising microalgae by high pressure homogenization. *Bioresource Technol* 2013; 140:165−171.
2. Mao HH, Moo-Young M. Disruption of baker's yeast by a new bead mill. *Biotechnol Tech* 1990; 4:335−340.
3. Zarraga IE, Taing R, Zarzar J, Luoma J, Hsiung J, Patel A, Lim F.High shear rheology and anisotropy in concentrated solutions of monoclonal antibodies. *J Pharm Sci* 2013; 102:2538−2549
4. Liu GR, Liu MB. *Smoothed Particle Hydrodynamics: A Meshfree Particle Method.* Singapore: World Scientific Publishing; 2003
5. Alexiadis A. A smoothed particle hydrodynamics and coarse-grained molecular dynamics hybrid technique for modelling elastic particles and breakable capsules under various flow conditions. *Int J Num Meth Eng* 2014; 100:713–719.
6. Pozrikidis C (Edited by) *Computational Hydrodynamics of Capsules and Biological Cells*: Boca Raton: Chapman & Hall, 2010.
7. Kumar A, Graham MD Mechanism of margination in confined flows of blood and other multicomponent suspensions *Phys. Rev. Lett.* 109:108102-6, 2012.
8. Kaoui B, Biros G, Misbah C Why do red blood cells have asymmetric shapes even in a symmetric flow? *Phys. Rev. Lett.* 103:188101-4, 2009.
9. Barthès-Biesel D *Microhydrodynamics and Complex Fluids*: Boca Raton: Chapman & Hall, 2012.
10. Morris JP, Fox PJ, Zhu Y. Modeling Low Reynolds Incompressible Flows Using SPH. *J Comput Phys* 1997; 136:214−226.
11. Müller M, Schirm S, Teschner M, Heidelberger B, Gross M. Interaction of fluids with deformable solids. *Comp Animat Virt W* 2004; 15:159−171
12. Coupier G, Farutin A, Minetti C, Podgorski T, Mishab C. Shape Diagram of Vesicles in Poiseuille Flow. *Phys Rev Lett* 2012; 180:1781061−5
13. Woolfenden HC, Blyth MG. Motion of a two-dimensional elastic capsule in a branching channel flow. *J Fluid Mech* 2011; 669:3−31
14. Secomb TW, Skalak R, Özkaya N, Gross JF. Flow of axisymmetric red blood cells in narrow capillaries. *J Fluid Mech* 1986; 163:405-−23
15. Quéguiner C, Barthes-Biesel D. Axisymmetric motion of capsules through cylindrical channels. *J Fluid Mech* 1997; 348:349−376